Langmuir
Article
pubs.acs.org/Langmuir

Chemically Modified Electrode with a Film of Nano Ruthenium Oxides Stabilizing High Valent RuO_4^- Species and Its Redox-Selective Sequential Transformation to Polynuclear Ruthenium Oxide-Metallocyanates

Annamalai Senthil Kumar,*[,†,‡] Tomoaki Tanase,[†] and Jyh-Myng Zen[§]

[†]*Department of Chemistry, Faculty of Science, Nara Women's University, Kitauoya-higashi-machi, Nara 630-8285, Japan,* [‡]*Department of Chemistry, Vellore Institute of Technology University, Vellore-632 014, India, and* [§]*Department of Chemistry, National Chung Hsing University, Taichung 40217, Taiwan*

Received June 21, 2009. Revised Manuscript Received August 7, 2009

High-valent $Ru^{VII}O_4^-$ (perruthenate) is a short-lived species in aqueous solutions (pH 1−14) and has scarcely been studied through electrochemistry. By a potential-controlled oxidative deposition method at 1 V vs Ag/AgCl using $RuCl_3$ in a pH 2 KCl-HCl buffer solution, chemically modified glassy carbon (GCE) and indium tin oxide (ITO) electrodes were successfully prepared with a film of hydrous nano ruthenium oxides RuO_2 and RuO_3, stabilizing the high-valent perruthenate anion (Ru(VII)-RuO_x-CME, $x = 2$ and 3, CME = chemically modified electrode). The electrodes showed three distinct redox peaks corresponding to Ru_2O_3/RuO_2, RuO_2/RuO_3, and RuO_4^{2-}/RuO_4^- redox processes at pH 2, like the classical RuO_2 electrodes in alkaline conditions. Solid state UV−visible spectra of the ITO/Ru(VII)-RuO_x-CME showed characteristic absorption very close to chemically generated authentic RuO_4^- species in alkaline solution. Further, redox-controlled sequential procedures yielded polynuclear ruthenium oxide-hexacyanometallate films (RuO-MCN-CME, M = Fe and Ru), in which Ru(VII)-RuO_x-CME acted as a specific template. A controlled-potential activation (>1 V) of Ru(VII)-RuO_x-CME, stabilizing the key RuO_4^- species, in a solution of $[Fe(CN)_6]^{3-}$ or $[Ru(CN)_6]^{4-}$, should be a critical step for the formation of polynuclear RuO-MCN matrix.

Introduction

Ruthenium heptavalent higher oxidation species, perruthenate ($Ru^{VII}O_4^-$), has excellent catalytic activity in organic media,[1] but due to its instability in aqueous solutions at pH 1−14,[2] to the best of our knowledge, there is no chemically modified electrode (CME) involving perruthenate, so far. In this work, new CMEs were established in which a high valent RuO_4^- species was stabilized by entrapping it into low valent hydrous nano ruthenium oxides (RuO_2 and RuO_3) (designated as Ru(VII)-RuO_x-CME, $x = 2$ and 3), taking $RuCl_3$ as the starting material by using potential-controlled anodic-oxidation deposition method. Further, a redox-controlled method formed a polynuclear ruthenium oxide−hexacyanometallate matrix on the CMEs (RuO-MCN-CMEs, M = Fe and Ru).

RuO-MCN (Scheme 1) has been emerged as an important class of inorganic materials with fusion of ruthenium oxide and Prussian Blue (PB; $M_i^{m+}[M'Fe(CN)_6]^{n-}$), which exhibit unusual physical and structural properties,[3−7] for instance, oxo-bridged dimetal units (Ru−O−Ru),[4] involvement of high-valent species,[6] strong acid stability,[6d] and superior electrocatalytic oxidative functions.[6,7] The RuO-MCN-CME has the ability to oxidize glucose,[6] *N*-nitrosoamine,[7i] and deoxyguanine[7m] in acidic aqueous solutions without any combination of enzymes. In addition, it is able to retain its network structure even in concentrated fuming acids including 14.4 M HNO_3, 12.1 M HCl, 18 M H_2SO_4, and 11.6 M $HClO_4$, while neither PB nor ruthenium oxide showed such interesting physical features.[6d] By utilizing its electrocatalytic activities, a wide variety of amperometric chemical sensors were developed with and without separation techniques suitable for industrial and biochemical sensing assays.[7] On the other hand, detailed information about the material has seldom been reported.[4,6a,d] In particular, the detailed mechanism for the RuO-MCN formation and structures of the redox-active ruthenium oxide species are unknown so far.

The RuO-MCNs were conventionally prepared by mixing of $RuCl_3 \cdot xH_2O$ and $[Fe(CN)_6]^{3-}$ or $[Ru(CN)_6]^{4-}$ in an acidic aqueous solution followed by electrochemical deposition (repeated cyclic voltammograms (E-cycle method) or potentiostatic methods (E_{app} method)) on a glassy carbon electrode

*Corresponding author. Telephone, +91-9976890675; E-mail, askumarchem@yahoo.com.

(1) (a) Hudlicky, M. *Oxidations in Organic Chemistry*; ACS: Washington, DC 1990. (b) Lee, D. G.; Congson, L. N. *Can. J. Chem.* **1990**, *68*, 774. (c) Murahashi, S.-I., Ed.; *Ruthenium in Organic Synthesis*; Wiley-VCH: Weinheim, Germany, 2004.(d) Ley, S. V.; Norman, J.; Grifith, W. P.; Marsden, S. P. *Synthesis* **1994**, 639.

(2) (a) Connick, R. E.; Hurley, C. R. *J. Am. Chem. Soc.* **1952**, *74*, 5012. (b) Silverman, M. D.; Levy, H. A. *J. Am. Chem. Soc.* **1954**, *79*, 3319. (c) Larsen, R. P.; Ross, L. E. *Anal. Chem.* **1959**, *31*, 176. (d) Lam, K. W.; Johnson, K. E.; Lee, D. G. *J. Electrochem. Soc.* **1978**, *125*, 1069.

(3) Cox, J. A.; Kulesza, P. J. *Anal. Chem.* **1984**, *56*, 1021.

(4) Cataldi, T. R. I.; Salvi, A. M.; Centonze, D.; Sabbatini, L. *J. Electroanal. Chem.* **1996**, *406*, 91.

(5) Kulesza, P. J.; Grzybowska, B.; Malik, M. A.; Chojak, M.; Miecznikowski, K. *J. Electroanal. Chem.* **2001**, *512*, 110.

(6) (a) Kumar, A. S.; Zen, J.-M. *ChemPhysChem* **2004**, *5*, 1227. (b) Kumar, A. S.; Zen, J.-M. *Electroanalysis* **2004**, *16*, 1211. (c) Kumar, A. S.; Chen, P.-Y.; Chien, S.-H.; Zen, J.-M. *Electroanalysis* **2005**, *17*, 210. (d) Kumar, A. S.; Zen, J.-M. *J.Mol.Catal.A.* **2006**, *252*, 63.

(7) (a) Wang, J.; Lu, Z. *Electroanalysis* **1989**, *1*, 517. (b) Cox, J. A.; Gray, T. J. *Anal. Chem.* **1989**, *61*, 462. (c) Cox, J. A.; Gray, T. J. *Anal. Chem.* **1990**, *62*, 2742. (d) Kennedy, R. T.; Huang, L.; Atkinson, M. A.; Dush, P. *Anal. Chem.* **1993**, *65*, 1882. (e) Gorski, W.; Cox, J. A. *Anal. Chem.* **1994**, *66*, 2771. (f) Cataldi, T. R. I.; Campa, C.; Centonze, D. *Anal. Chem.* **1995**, *67*, 3740. (g) Cox, J. A.; Alber, K. S.; Brockway, C. A.; Tess, M. E.; Gorski, W. *Anal. Chem.* **1995**, *67*, 993. (h) Cataldi, T. R. I.; Centonze, D.; Guerrieri, A. *Anal. Chem.* **1995**, *67*, 101. (i) Gorski, W.; Cox, J. A. *J. Electroanal. Chem.* **1995**, *389*, 123. (j) Cox, J. A.; Cheng, L. Electrocatalytic determination of biochemical compounds. In *Electroanalytical Methods for Biological Materials*; Brajter-Toth, A., Chambers, J. Q., Ed.; Marcel Dekker: New York, 2002; p 417. (k) Chen, S.-M.; Hsueh, S.-H. *J. Electroanal. Chem.* **2004**, *566*, 291. (l) Chen, S.-M.; Lu, M.-F.; Lin, K.-C. *J. Electroanal. Chem.* **2005**, *579*, 163. (m) Paixão, T. R. L. C.; Bertotti, M. *Electrochim. Acta* **2007**, *52*, 2181. (n) Chu, H.-W; Thangmuthu, R; Chen, S.-M. *Electrochim. Acta* **2008**, *53*, 2862. (o) Paixão, T. R. L. C.; Bertotti, M. *J. Pharm. Biomed. Anal.* **2008**, *46*, 528.

Scheme 1. (I) Estimated Active Site Structure for the Polynuclear RuO-MCN (M = Fe or Ru)[6a] and Its Simplified Representative View; (II) Dynamic of Naked and ITO/Chemically Modified Ruthenium Oxide Species under Various Chemical (A) and Electrochemical Conditions (B & C) in a pH 2 KCl-HCl Solution at Room Temperature[a]

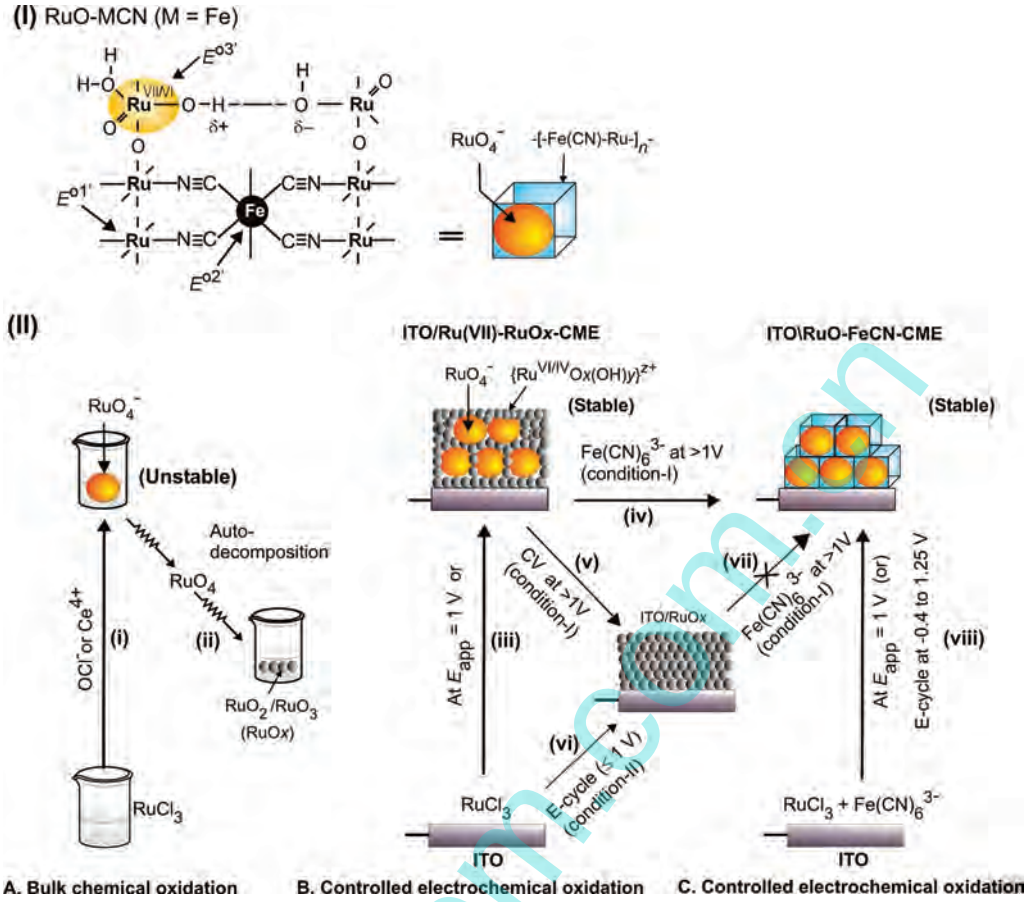

[a] (A) Chemical oxidation. (B) Sequential steps based preparation of ITO/RuO-FeCN-CME through cases (iii) and (iv). (C) Conventional preparation step for ITO/RuO-FeCN-CME (case viii).[4] $E^{o1'}$, $E^{o2'}$, and $E^{o3'}$ correspond to the standard electrode potentials of the ITO/RuO-FeCN-CME.

(GCE) surface (Scheme 1(II)C, step (viii)).[4] Recently, a hybridized RuO-MCN/silicamolybdate matrix film was also prepared using the conventional procedure along with a silicamolybdate ($SiMo_{12}O_{40}^{4-}$) dissolved solution.[8] Meanwhile, few template-assisted PB analogues by sequential formation procedures (either by chemical or electrochemical) were reported in the literature, with template examples being poly(vinylpyrrolidone)-protected Fe^{3+},[9a] bis[3-(triethoxysily) propyl]tetrasulfide sol−gel-modified Fe^{3+},[9b] Fe^{3+}-adsorbed gold,[9c] Fe^{3+}-enriched industrial ash,[9d] protonated polyimmidoamine dendrimer with sol−gel-modified $[Fe(CN)_6]^{3-}$,[9e] and azobenzene containing cationic vesicle-modified $[Fe(CN)_6]^{3-}$.[9f] To the our best knowledge, no such sequential technique is discovered for the case of RuO-MCN. Unfortunately, Ru^{3+} ion is unstable and exists as a complicated oxy/hydroxy ruthenium species in aqueous solutions.[10] $Ru^{IV}O_2$ is a stable ruthenium oxide (well−known material used for electrochemical capacitor);[11] however, it might be difficult to further modify the RuO_2 surfaces. In this work, we systematically investigated the preparation and characterization of the Ru(VII)-RuO_x-CME, and it was utilized for redox-controlled sequential step formation of the RuO-MCN-CME films.

Experimental Procedures

Aqueous solution containing gaseous RuO_4 species at ~5 °C (0.5%, Sterm Chemical, USA), tetrapropylammonium perruthenate ($[nPr_4N][RuO_4]$, Aldrich), $RuO_2 \cdot xH_2O$ (Sterm Chemical), $RuCl_3 \cdot xH_2O$ (Ru content 38.9%, Tanaka Metal Company, Tokyo), potassium ferricyanide (Kanto Chemical, Japan), potassium cyanoruthenate (Aldrich) and all other chemicals employed were of analytical grade and used without further purification. Aqueous solutions were prepared with doubly deionized water. Unless specified, all the electrochemical measurements were carried out in a KCl-HCl (I = 0.1 M) buffer solution at pH 2. ***Caution!*** *RuO_4^- in acidic solution generates gaseous RuO_4 species, which is likely to be deposited on biological tissue if inhaled. Note that RuO_4 solutions are readily decomposed at room temperature. Special care must be taken during handling the solutions.*

(8) Chen, S.-M.; Song, J.-L. *J. Electroanal. Chem.* **2007**, *599*, 41.
(9) (a) Uemura, T.; Kitagawa, S. *J. Am. Chem. Soc.* **2003**, *125*, 7814. (b) Guo, Y.; Guadalupe, A. R.; Resto, O.; Fonseca, L. F.; Weisz, S. Z. *Chem. Mater.* **1999**, *11*, 135. (c) Millard, R. C.; Madden, C. E.; Sutherland, I.; Mortimer, R. J.; Fletcher, S.; Marken, F. *Chem. Commun.* **2001**, 1994. (d) Kumar, A. S.; Chen, P.-Y; Zen, J.-M. *Electroanalysis* **2004**, *16*, 242. (e) Zamponi, S.; Kijak, A. M.; Sommer, A. J.; Marassi, R.; Kulesza, P. J.; Cox, J. A. *J. Solid State Electrochem.* **2002**, *6*, 528. (f) Einaga, Y.; Sato, O.; Iyoda, T.; Fujishima, A.; Hashimoto, K. *J. Am. Chem. Soc.* **1999**, *121*, 3745.
(10) (a) Cotton, F. A.; Willikinson, G. *Advanced Inorganic Chemistry*; Wiley: New York, 1988; p 868. (b) Inzelt, G.; Puskás, Z. *Electrochem. Commun.* **2004**, *6*, 805. (c) Santos, M. C.; Terezo, A. J.; Fermandes, V. C.; Pereira, E. C.; Bulhões, L. O. S. *J. Solid State Electrochem.* **2005**, *9*, 91.
(11) (a) Chang, K.-H.; Hu, C.-C. *J. Electrochem. Soc.* **2004**, *151*, A958. (b) Hu, C.-C.; Huang, Y.-H. *J. Electrochem. Soc.* **1999**, *146*, 2465. (c) Hu, C.-C.; Chiang, H.-R.; Wang, C.-C. *J. Solid State Electrochem.* **2003**, *7*, 477. (d) Park, B.-O.; Lokhande, C. D.; Park, H.-S.; Jung, K.-D.; Joo, O.-S. *J. Mater. Sci.* **2004**, *39*, 4313. (e) Kvastek, K.; Horvat-Radoševic, V. *J. Electroanal. Chem.* **2001**, *511*, 65. (f) Vigier, F.; Gloaguen, F.; Léger, J. M.; Lamy, C. *Electrochim. Acta* **2001**, *46*, 4331. (g) Anderson, D. P.; Warren, L. F. *J. Electrochem. Soc.* **1984**, *131*, 347. (h) Jow, J.-J.; Lee, H.-J.; Chen, H.-R.; Wu, M.-S.; Wei, T.-S. *Electrochim. Acta* **2006**, *52*, 2625.

Electrochemical experiments were carried out with a Hokuto Denko HZ-3000 (Japan) electrochemical workstation at room temperature (25 ± 2 °C). A three-electrode assembly consists of a platinum wire counter, a Ag/AgCl saturated KCl reference, and a GCE (geometrical surface area = 0.07 cm^2, Bioanalytical System (BAS)), indium tin oxide (ITO) plate (approximately 1 cm × 4 cm, Kinoene Optical Industry, Tokyo, Japan), or its CMEs as working electrodes. N_2 purged (20 min) solutions were used for electrochemical and UV−visible (UV−vis) spectroscopic studies. Cyclic voltammetry (CV) experiments were all measured starting from its rest potential (E_{rest}) to the desired potential window. An inbuilt program is available with the electrochemical instrument to measure the E_{rest} value of a three-electrode system. Ex situ atomic force microscopic (AFM) analyses were carried out by using a CSPM4500 (China) instrument.

Prior to the CME preparations, the GCE surface was mechanically polished with a BAS polishing kit followed by sonication for about 3 min in double distilled water and then electrochemically pretreated within a −0.2 to 1.2 V window for a continuous six cycles. Conventional RuO-FeCN or RuO-RuCN films were prepared by repeated potential−cycling methods on the GCE or ITO surfaces (qualitatively similar CV response) in a solution containing Ru^{3+} and $Fe(CN)_6^{3-}$ or $Ru(CN)_6^{4-}$ (2 mM for each ion) at pH 2.[4]

Ru(VII)-RuO_x-CME films were prepared on GCE or ITO surfaces by potentiostatic oxidative-deposition method (i.e., E_{app} method) at an applied potential (E_{app}) of 1 V vs Ag/AgCl (optimal) for 900 s in a KCl-HCl solution of $RuCl_3$ (2 mM) at pH 2. Repeated potential−cycling method (E-cycle method) with a window of −0.4 to 1.25 V vs Ag/AgCl in a KCl-HCl solution of $RuCl_3$ (2 mM) at pH 2 at a scan rate (v) of 50 mV/s (total 21 cycles) was also used to prepare the Ru(VII)-RuO_x-CMEs. However, the latter method resulted in relatively less-reactive ruthenium oxide surfaces. Unless stated, the Ru(VII)-RuO_x-CME used in this work was prepared by the potentiostatic oxidative-deposition method only.

RuO-MCN-CMEs (M = Fe and Ru) were prepared according to the new sequential steps as shown in Scheme 1(II)B (steps (iii) and (iv)); the Ru(VII)-RuO_x-CME film was used as a template material in a solution of $Fe(CN)_6^{3-}$ or $Ru(CN)_6^{4-}$ at pH 2 with 5 continuous CV cycles at a scan rate of 50 mV/s in a potential window of −0.4 to 1.25 V vs Ag/AgCl.

Solid state and solution phase UV−vis spectra were recorded with an Agilent 8453E UV−vis spectroscopy system (Germany). Fourier transform infrared (FTIR) measurments were carried out by the KBr pellet method using a JASCO FT/IR-410 instrument (Japan). For FTIR measurements, the Ru(VII)-RuO_x films were prepared on ITO electrodes (working area ∼1 cm^2) using 10 mM $RuCl_3$ as the starting material under the optimal condition. Prior to the measurements, samples were washed with water, then dried in an oven (∼100 °C) for ∼5 min and in air for 1 h. Scratched samples were further tested for FTIR with a KBr pellet method.

A simplified equation of $E_{RHE} = [(E_{Ag/AgCl} + 0.06pH) + E^{o}_{Ag/AgCl}$ (0.22)]/V vs Ag/AgCl was used for conversion of the reference potentials between $E_{Ag/AgCl}$ and E_{RHE} (RHE = reversible hydrogen electrode).

Results and Discussion

Preparation of Ru(VII)-RuO_x-CME. The CME was prepared by using a solution of $RuCl_3$ (2 mM) as the starting material at pH 2 with potentiostatic (E_{app} method) or potential cycling (E-cycle method) oxidative-deposition techniques. Figure 1A,B shows typical responses of the potentiostatic method at an applied potential (E_{app}) of 1 V vs Ag/AgCl with a deposition time, t_{Dep} = 900 s and of the E-cycle method in a window of −0.4 to 1.25 V vs Ag/AgCl at v = 50 mV/s for 21 cycles, respectively. The CMEs were stable in air under pH 2 open-circuit solution conditions. The former preparation method (E_{app} method) showed an L-shaped current−time response, where the deposition current sharply decreases up to 100 s, after which it tends to plateau (Figure 1A). In the latter E-cycle approach, a well-defined anodic peak with increased current up to 10 min at 1.1 V was observed, which was then found to saturate. The redox peak appears with a quasi-reversible characteristic ($i_{pc}/i_{pa} \sim 0.2$) centered at 0.960 V vs Ag/AgCl (Figure 1B). Figure 1C,D shows the first CV responses of the freshly prepared respective CMEs in KCl-HCl solution at pH 2. The potentiostatically prepared CME showed a E_{rest} value of 0.9 ± 0.03 V vs Ag/AgCl. Further forward CV cathodic scans yielded two defined reduction redox peaks at 0.750 V (E_{pc}^2) and 0.210 V vs Ag/AgCl (E_{pc}^1) (enlarged view in Figure 1C), and the corresponding anodic reverse scan showed respective counter peaks at E_{pa}^1 = 0.354 (0.694 V vs RHE), E_{pa}^2 = 0.840 V (1.18 V vs RHE) along with an intense oxidation peak at E_{pa}^3 = 1.11 V (1.45 V vs RHE) and its counter peak at 0.846 V vs Ag/AgCl (E_{pc}^3) at the beginning of the second cathodic cycle. Repeated experiments with an ITO electrode also resulted in qualitatively similar CV patterns. The observed anodic redox potentials for the present CMEs (E_{pa}^1, E_{pa}^2, and E_{pa}^3 of 0.69, 1.18, and 1.45 V vs RHE, respectively) are in accord with the reported standard electrode potentials for RuO_2-modified electrodes in alkaline solutions, $Ru^{III}_2O_3/Ru^{IV}O_2$ (E^{o1}), $Ru^{IV}O_2/Ru^{VI}O_3$ (E^{o2}), and $Ru^{VI}O_4^{2-}/Ru^{VII}O_4^{-}$ (E^{o3}) corresponding to 0.5, 1.15, and 1.45 V vs RHE, respectively.[12] The result indicated the existence of three different electroactive species: hydrous RuO_2 and RuO_3 (or RuO_4^{2-}) as well as RuO_4^{-} within the surface matrix of the CMEs. Electroactive surface Ru(n+) concentrations, $\Gamma_{Ru(n+)}$, were calculated for the Ru(IV), Ru(VI), and Ru(VII) species from the corresponding anodic CV peaks as 10.6, 0.30, and 70 nmol/cm^{-2}, respectively, based on the equation $Q_{pa} = nFA\Gamma_{Ru(n+)}$ (Q_{pa} = area under the anodic peak at v = 10 mV/s, n = number of electrons involved, F = faradic constant, and A = geometric surface area), further indicating the relative ratios ($\Gamma_{Ru(n+)}/\Gamma_{Ru(IV)} + \Gamma_{Ru(VI)} + \Gamma_{Ru(VII)}$) of 13%, 0.5%, and 86.5% for the Ru(IV), Ru(VI), and Ru(VII) sites, respectively (Table 1). The redox peaks occurring in the CV process could be due to electrogenerated and/or fractions of real compounds. On the basis of the E_{rest} and the CV results, we initially speculate that the real compounds of the CME matrix mainly consisted of $Ru^{VII}O_4^{-}$ supported by a considerable amount of hydrous RuO_2 with trace amounts of RuO_3 species. The CME prepared by the E-cycle method showed a qualitatively similar CV pattern, but the current response was decreased 8-fold relative to the CME prepared by the E_{app} method (Figure 1D, Table 1). The existence ratios for electroactive hydrous Ru oxide species are 25%, 1.5%, and 73.5%, respectively, for the RuO_2, RuO_3 and RuO_4^{-} sites, which are appreciably different from those of the CME prepared by the E_{app} method (Table 1). All these observations indicated the formation of mixed-valent ruthenium oxide species during the oxidative-anodic deposition procedures, and, among them, the E_{app} preparation method proved to be effective to produce the highly concentrated Ru(VII) species. Later AFM analyses support this observation. In light of the real ruthenium compositions, we assumed a model for the surface of Ru(VII)-RuO_x-CME, where high-valent reactive RuO_4^{-} species were stabilized in the three-dimensional (3D) network of protonated hydrous ruthenium oxide (RuO_2) (Scheme 1(II)B). Spectrochemical and AFM

(12) (a) Bard, A. J.; Parsons, R.; Jordan, J. *Standard Potentials in Aqueous Solutions*; IUPAC; Marcel Dekker: New York, 1983; p 413. (b) Burke, L. D.; Murphy, O. J. *J. Electroanal. Chem.* **1980**, *109*, 199. (c) Burke, L. D.; Healy, J. F. *J. Electroanal. Chem.* **1981**, *124*, 327. (d) Lyons, M. E. G.; Burke, L. D. *J. Chem. Soc., Faraday Trans. I* **1983**, *83*, 299. (e) Kumar, A. S.; Pillai, K. C. *J. Solid State Electrochem.* **2000**, *4*, 408.

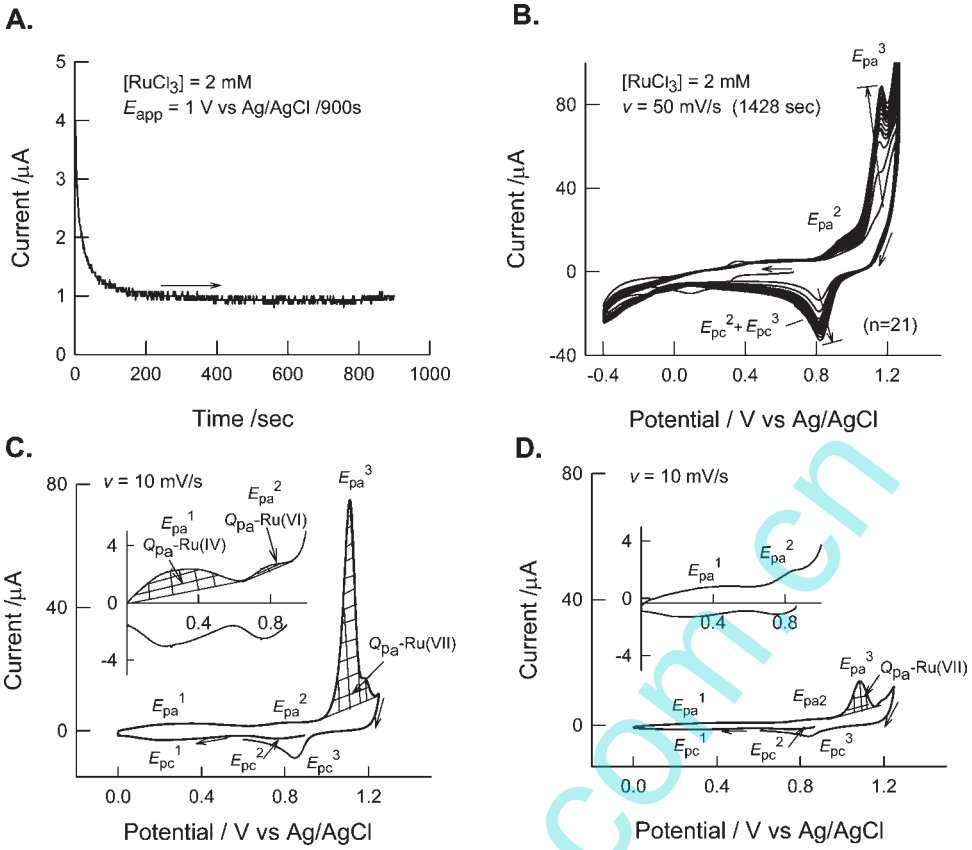

Figure 1. Electrochemical responses of a GCE with 2 mM $RuCl_3$ in a pH 2 KCl-HCl buffer solution by (A) potentiostatic deposition at E_{app} = 1 V vs Ag/AgCl for 900s and (B) repetitive E-cycle in a deposition window of −0.4 to 1.25 V vs Ag/AgCl at a scan rate (v) of 50 mV/s (n = 21). First CV cycle responses of GCE/Ru(VII)-RuO_x-CME prepared by (C) potentiostatic and (D) E-cycle deposition methods in pH 2 KCl-HCl at a v = 10 mV/s. Inset figures in C and D correspond to an enlarged version of a lower potential window.

Table 1. Surface Redox Feature of GCE/Ru(VII)-RuO_x-CMEs Prepared at Different Methods in pH 2

redox species	E^o,[a] mV vs Ag/AgCl	ΔEp,[b] mV	E_{pa}, mV vs Ag/AgCl	E_{pa}, mV vs RHE	j_{pa} ($\mu A \cdot cm^{-2}$)	Q_{pa}, μC	$\Gamma_{Ru(n+)}$, nmoles·cm^{-2c} [relative %][d]
(A) E_{app} = 1 V vs Ag/AgCl for 900 s Prepared							
1. Ru_2O_3/RuO_2 (E^{o1})	282	144	354	694	24.9	72.03	10.60 [13%] of Ru(IV)
2. RuO_2/RuO_3 (E^{o2})	794	90	840	1180	4.8	3.98	0.30 [0.5%] of Ru(VI)
3. RuO_4^{2-}/RuO_4^- (E^{o3})	978	264	1110	1450	970.4	477.53	70.00 [86.5%]of Ru(VII)
(B) E-Cycle at −0.4 to 1.25 V vs Ag/AgCl (n = 21) Prepared							
1. RuO_2/Ru_2O_3 (E^{o1})	241	230	356	696	7.8	23.70	3.50 [25%] of Ru(IV)
2. RuO_3/RuO_2 (E^{o2})	772	95	819	1159	2.5	1.54	0.13 [1.5] of Ru(VI)
3. RuO_4^-/RuO_4^{2-} (E^{o3})	965	250	1090	1430	130.8	70.40	10.32 [73.5%]of Ru(VII)

[a] $E^o = (E_{pa} + E_{pc})/2$. 1st cycle CV at v = 10 mV/s. [b] $\Delta Ep = E_{pa} - E_{pc}$. [c] Electroactive surface species, $\Gamma_{Ru(n+)}$ = surface Ru concentration (anodic) calculated using the equation $Q_{pa} = nFA\Gamma_{Ru(n+)}$ (A = 0.0707 cm^2). [d] $(\Gamma_{Ru(n+)}/(\Gamma_{Ru(IV)} + \Gamma_{Ru(VI)} + \Gamma_{Ru(VII)}) \times 100)$. E^{o1}, E^{o2}, and E^{o3} correspond to standard electrode potentials of the GCE/Ru(VII)-RuO_x-CMEs.

studies of the material provide supportive information for the real surface species and the nanosize of system in a later section. The detailed characterization will be described in the following section.

Irrespective of the preparation methods, the Ru(VII)-RuO_x-CME showed critical stability features depending on the working CV windows. The CVs in an anodic potential window (>1 V (condition I)) led to slow decomposition of the surface materials (Figures S1A(a) and S1B(a)). On the other hand, the CVs in a restricted window (≤1 V (condition II)) showed highly stable responses (Figures S1A(b) and S1B(b)). No marked alteration in the peak current and peak potential of even prolonged cycles (n = 20) indicated appreciable stability of the Ru(VII)-RuO_x-CME in the window (condition II). It is notable that the potential window of condition II involves only the RuO_2 and RuO_3 redox processes, while that with condition I covers the high-valent RuO_4^- redox process. Electrochemical activation of the high-valent RuO_4^- species could result in decomposition of the surface compounds.

The E_{app} method was found to be characteristic and specific for preparation of the Ru(VII)-RuO_x-CMEs. The CME formation experiments were carried out at different E_{app} conditions discretely from −0.4 to 1.3 V vs Ag/AgCl. The i_{pa}^3 current responses of the first CV cycling (condition I) were uniformly monitored, as shown in Figure 2, to show a sharp i_{pa}^3 behavior against the E_{app} with an optimal point at E_{app} = 1 V vs Ag/AgCl. The E_{app} below 0.8 V or over 1.2 V vs Ag/AgCl resulted in only a trace amount of

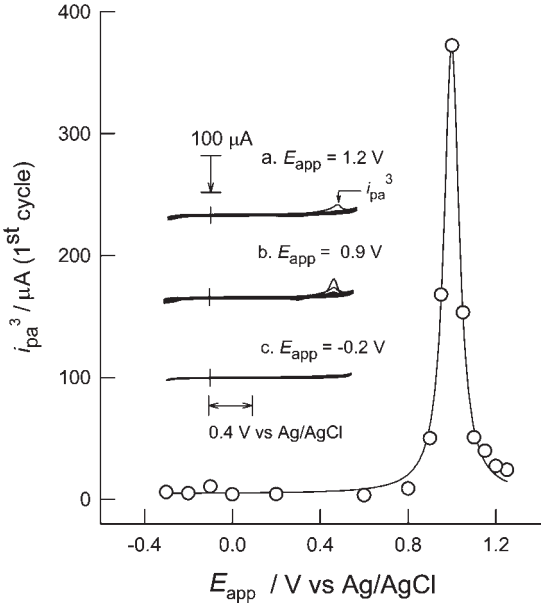

Figure 2. Plot of high-valent anodic peak current (i_{pa}^3) against applied potential (E_{app}) preparation of GCE/Ru(VII)-RuO_x-CME in a pH 2 KCl-HCl. Deposition time (t_{Dep}) = 900 s. First CV cycle response is uniformly taken for quantitative analysis. Inset figures correspond to representative CV responses of GCE/Ru(VII)-RuO_x-CME prepared at E_{app} = −0.2 V (a), 0.9 V (b), and 1.2 V vs Ag/AgCl (c).

the Ru(VII)-RuO_x-CME formation (inset CVs in Figure 2). The quantitative i_{pa}^3 response at E_{app} = 1 V vs Ag/AgCl was ∼400 times higher than that with E_{app} = 0.8 V vs Ag/AgCl. The optimal potential E_{app} = 1 V vs Ag/AgCl was found to be a critical condition for the $RuCl_3$ oxidative deposition into the Ru(VII)-RuO_x-CME in which the high-valent RuO_4^- species is stabilized.

Characterization of the Ru(VII)-RuO_x-CME. Formation of the RuO_4^- species within the ruthenium oxide matrix of the CME in a pH 2 solution is unusual, since the naked Ru(VII) species were reported to be highly unstable in aqueous solution of pH 1−14 as a result of complicated disproponation and decomposition reactions.[2,12a] Solution- and solid-state UV−vis spectral data for high-valent ruthenium species with various conditions and systems reported previously and in this work are summarized in Table S1. The RuO_4^- can be relatively stable in a strong alkaline solution of 4 M KOH with a characteristic UV−vis peak at 310 and 385 nm (entry 5, Table S1).[2a,c] Mixing with an oxidant such as OCl^- and Ce^{4+} in a dilute alkaline solution, $RuCl_3$ also generated RuO_4^-, and it can survive in the medium depending upon the excess oxidant concentration (entries 6 and 7, Table S1).[2a−c] In acidic pHs, RuO_4^- decomposed rapidly. A solution (pH 2) of a few milligrams of [nPr$_4$N][RuO_4] immediately exhibited characteristic UV−vis patterns at ∼310 and 386 (vibrational) nm, indicating formation of the oxidized $Ru^{VIII}O_4$ species (entry 3 in Table S1, Figure 3A(a)),[2a] and further standing of the solution overnight in air resulted in a clear solution (entry 4 in Table S1, Figure 3A(b)) with complete decomposition into stable RuO_2 and RuO_3 (case (ii) in Scheme 1(II)A). It is interesting to notice that the Ru(VII)-RuO_x-CME is stable in a pH 2 solution with the open-circuit condition and with the CV condition II (Figure S1A(b)). It can be estimated that the lower valent hydrous metal oxides, RuO_2 and RuO_3, are able to protect the RuO_4^- species within the 3D network through Ru−O−Ru, hydrogen bonding, and electrostatic interactions against conventional disproportionation and decomposition reactions. Perhaps it can be decomposed under CV condition I (>1 V), as a result of the large amount of bulk proton insertion reactions and, in turn, facilitate disproportionation and destabilization of the matrix.

We also collected other qualitative evidence for the existence of the RuO_4^- species within the Ru(VII)-RuO_x-CME matrix (Table S1, Figures 3B and 4). At first, freshly prepared Ru-(VII)-RuO_x-CME was found to selectively oxidize D-glucose at 1.11 V vs Ag/AgCl in pH 2 (1.45 V vs RHE) (Figure 3B), demonstrating an existence of RuO_4^-, which is similar to the electro-generated RuO_4^- species at 0.40 V vs Ag/AgCl in alkaline condition (1.46 V vs RHE) with RuO_2 electrodes.[13] In this work, however, the Ru(VII)-RuO_x-CME response decreased with repeated CV cycles. Notably, the naked RuO_2 electrodes in a pH 2 condition failed to show any such oxidation catalysis toward glucose.[6b,d] The IR spectra of Ru(VII)-RuO_x-CME showed a characteristic peak at 799 cm^{-1} corresponding to Ru=O species,[14a−d] along with very broad peaks in 1624−1077 cm^{-1} ascribable to water, hydroxo-, and oxo-bridged species[14e] involved in the film matrix (Figure 4B). Control IR spectrum with commercial $RuO_2 \cdot xH_2O$ did not show any Ru=O characteristic peaks around 800 cm^{-1}, while a broad shoulder centered at the high frequency region of 3380 cm^{-1} (not shown) and a low frequency peak pf ∼500 cm^{-1} were noticed due to a hydrous RuO_2 (Figure 4B(a)). While high-temperature prepared RuO_2 and RuO_2(110) crystalline materials were also reported for strong −OH surface peaks at ∼ 3000 cm^{-1} along with a {$Ru_3(\mu_3$-O)} lattice feature at ∼500 cm^{-1},[14f,g] the Ru=O functional groups were never reported with classical RuO_2 samples. The ITO/Ru(VII)-RuO_x-CME was directly subjected for solid-state UV−vis characterization as in Figure 4C(a) (entry 10 in Table S1). Interestingly, the materials show characteristic peaks at 309 and 390 nm corresponding to RuO_4^-,[2a−c] along with a broad shoulder at ∼600 nm due to the discrete RuO_x materials with Ru−O−Ru (i.e.,{$Ru_2(\mu_2$-O)}) network.[15] Control experiments for a solution of RuO_4^- in 0.1 M NaOH/OCl^- showed similar UV−vis spectral peaks at 310 and 387 nm (Figure 4C(b), entries 6 and 7 in Table S1), while a ITO/RuO_x-CME capacitor film prepared by the conventional E-cycle in the window of −0.2 to 1.0 V vs Ag/AgCl with $RuCl_3$ in pH 2 showed an unidentified UV−vis feature (observed at 397 and ∼600 nm, presumably due to the fraction of Ru(IV) and Ru(VI) with Ru−O−Ru (entry 12 in Table S1). In addition, a possible Ru−O−Ru redox network structure could be composed of Ru^{III}−O−Ru^{III}, Ru^{IV}−O−Ru^{IV} and Ru^{III}−O−Ru^{IV}. The point of zero surface charge (pH_{PZC}) of RuO_2 powder samples was reported at pH ∼5.[16] Below that pH, the RuO_2 exists in protonated forms as $Ru^{IV/VI}O_x(OH)_y^{z+}$ (where $0 < z < 1$). Hence this work shows that, at pH 2, the protonated hydrous ruthenium(IV) oxides could electrostatically stabilize the

(13) (a) Dharuman, V.; Pillai, K. C. *J. Solid. State Electrochem.* **2006**, *10*, 967. (b) Lyons, M. E. G.; Lyons, C. H.; Michas, A.; Bartlett, P. N. *Analyst* **1992**, *117*, 1271.
(14) (a) Green, G.; Griffith, W. P.; Hollinshead, D. M.; Ley, S. V.; Schröder *J. Chem. Soc. Perkin Trans. I* **1984**, 681. (b) Che, C.-M.; Tang, W.-T.; Lee, W.-O.; Wong, W.-T.; Lai, T.-F. *J. Chem. Soc., Dalton Trans.* **1989**, 2011. (c) Dangel, A. C.; El-Hendawy, A. M.; Griffith, W. P.; O'Mahoney, C. A.; Williams, D. J. *J. Chem. Soc., Dalton Trans.* **1990**, 737. (d) Yukawa, Y.; Aoyagi, K.; Kurihara, M.; Shirai, K.; Shimizu, K.; Mukaida, M.; Takeuchi, T.; Kakihana, H. *Chem. Lett.* **1985**, 283. (e) Nakamoto, K. *Infrared and Raman Spectra of Inorganic and Coordination Compounds*, 3rd ed., John Wiley & Sons: New York, 1978. (f) Musić, S.; Popovic, S.; Maljković, M.; arić, A. *Mater. Lett.* **2004**, *58*, 1431. (g) Wang, J.; Fan, C. Y.; Sun, Q.; Reuter, K.; Jacobi, K.; Scheffler, M.; Ertl, G. *Angew. Chem. Int. Ed.* **2003**, *42*, 2151.
(15) (a) Llobet, A.; Curry, M. E.; Evans, H. T.; Meyer, T. J. *Inorg. Chem.* **1989**, *28*, 3131. (b) Das, B. K.; Chakravarty, A. R. *Inorg. Chem.* **1990**, *29*, 2078. (c) Kumar, A. S.; Tanase, T.; Iida, M. *Langmuir* **2007**, *23*, 391.
(16) (a) Trasatti, S. In *The Electrochemistry of Novel Materials*; Lipkowski,J., Ross, P. N., Eds.; VCH: New York, 1998; Vol. *44*, p 1481. (b) Trasatti, S. *Electrochem. Acta* **2000**, *45*, 2377. (c) Guerrini, E.; Trasatti, S. *Russ. J. Electrochem.* **2006**, *42*, 1017.

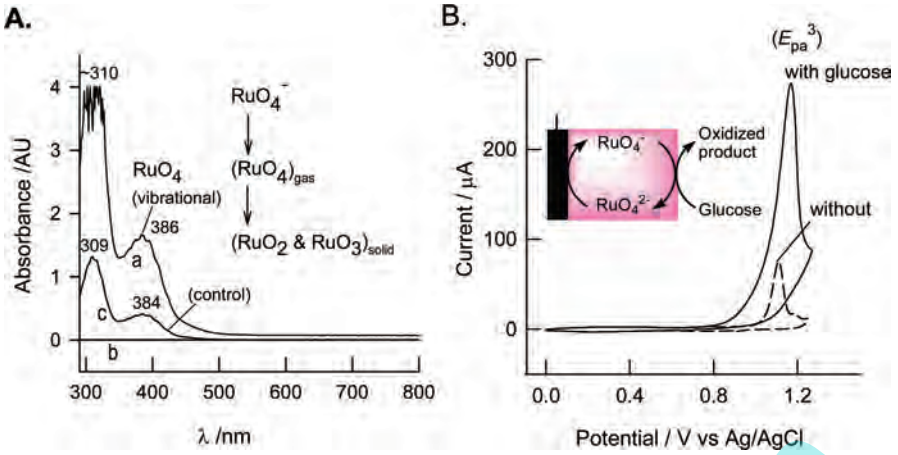

Figure 3. (A) UV−vis response of [nPr$_4$N][RuO$_4$] (2 mM) immediately (a) and after 12 h (b) in pH 2 KCl-HCl buffer solution. For case (b), a clear layer is further subjected for the analysis. (c) Control RuO$_4$ dissolved ice-cold water (50 μL of 0.5% solution diluted to 3 mL water). (B) Typical CV response (1st cycle) of GCE/Ru(VII)-RuO$_x$-CME without and with 100 mM of glucose at v = 10 mV/s in pH 2 KCl-HCl buffer solution. Inset figure shows the redox mechanism for the glucose oxidation reaction.

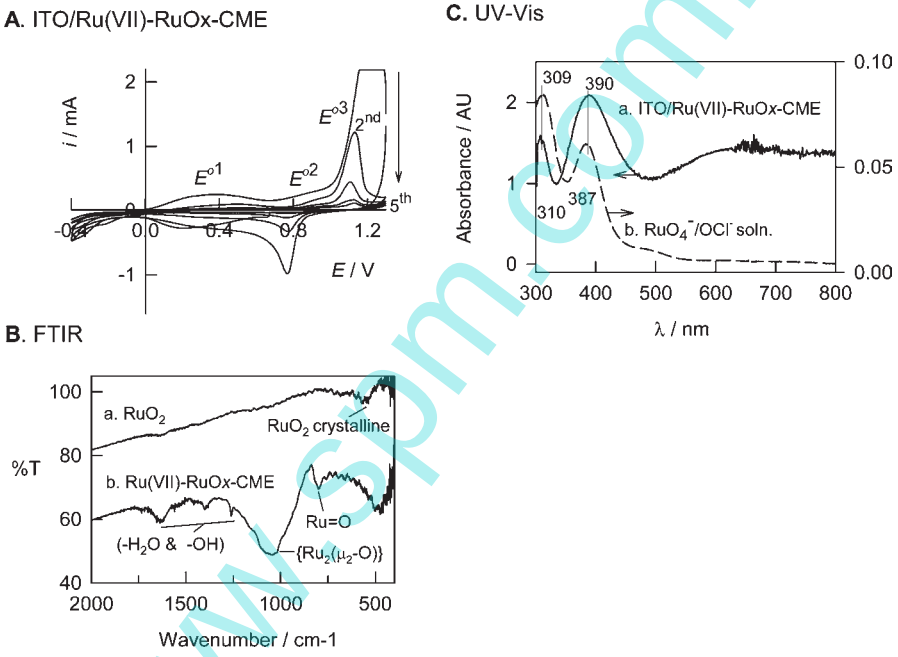

Figure 4. (A) Repetitive CV response of a ITO/Ru(VII)-RuO$_x$-CME at v = 50 mV/s in pH 2 KCl-HCl. (B) FTIR spectrum of Ru(VII)-RuO$_x$-CME and commercial RuO$_2$. (C) (a) solid state UV−vis spectra of ITO/Ru(VII)-RuO$_x$-CME and (b) solution phase UV−vis spectra of RuO$_4^-$ in 0.1 M NaOH/NaOCl solution.

anionic RuO$_4^-$ species within the Ru(VII)-RuO$_x$-CME matrix as shown in the Scheme 1(II)B.

Figure 5 shows typical AFM images of ITO/Ru(VII)-RuO$_x$-CMEs, prepared by E_{app} and E-cycle methodologies. A large number of high intense islands with an average particle size of ~300 nm and a few less intense islands with particle size of ~200 nm were observed, respectively, for the E_{app} and E-cycle prepared electrodes, which are in parallel to the corresponding voltammetric current values as in Figure 1C,D. These nano islands are expected to be the active site of the high-valent ruthenium species stabilized by low valent ruthenium oxides particulate system, which was identified from previous electrochemical, electrocatalytic, UV−vis, and FTIR studies.

Hydrous ruthenium oxides were often prepared using E-cycle (≤1 V vs Ag/AgCl),[11a−d] galvanostatic,[11e] and cathodic deposition[11f] methods with the aim of capacitor applications on Ti-based supporting materials, since it can form a solid-solution (alloy) with ruthenium oxides.[16] Although the potentiostatic approach based on oxidative deposition of ruthenium oxides was very few,[11g,h] Anderson and Warren prepared a Pt/RuOx(OH)y electrode at an applied potential of 0.9 V vs SCE using a chemically generated [Ru(η^6-C$_6$H$_6$)(OH)$_3$]$^{2+}$ precursor complex in pH 5 solution.[11g] Jow et al. reported a Ti/RuO$_x$(OH)$_y$ electrode using RuCl$_3$ as a starting material by an oxidative electrochemical deposition similar to the present optimal case.[11h] The authors believed that the electrode was composed of a hydrous RuO$_2$ and RuO$_3$ mixture, determined by X-ray photoelectron spectroscopy (XPS) and scanning electron microscopy (SEM).[11h] Kim and Winograd pointed out that naked high-valent species such as RuO$_4^-$ and RuO$_4$ were discharged under a strong electron-beam during normal XPS measurements[17] and

(17) Kim, K. S.; Winograd, N. *J. Catal.* **1974**, *35*, 66.

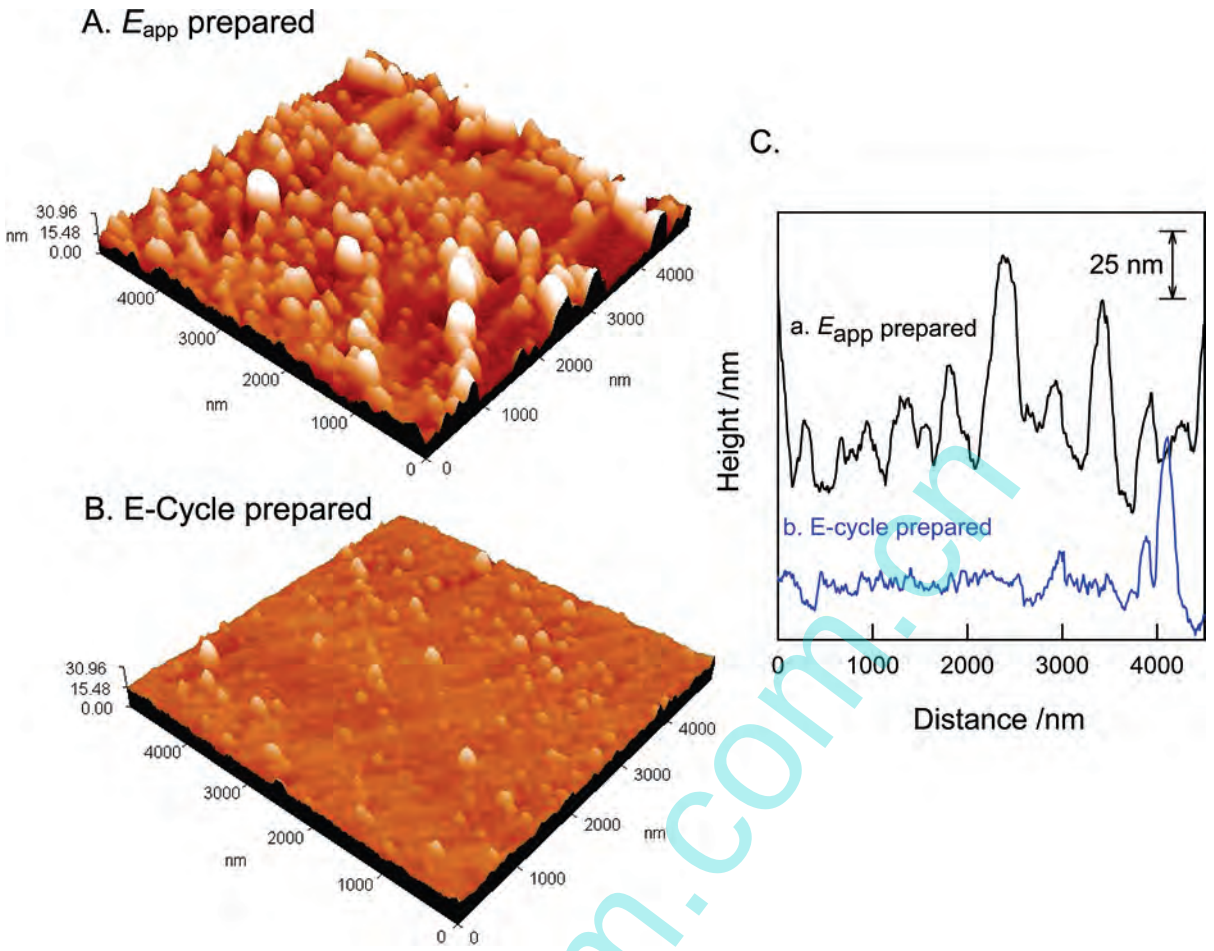

Figure 5. AFM images of the ITO/Ru(VII)-RuO_x-CMEs, prepared by (A) E_{app} at 1 V vs Ag/AgCl for 900s and (B) E-cycle at −0.4 to 1.25 V vs Ag/AgCl (n = 21) methods using 2 mM $RuCl_3$ in pH 2 KCl-HCl buffer solution (C) and its typical two-dimensional (2D) topographies.

further converted to decomposed species, RuO_2 and RuO_3 (e.g., with a RuO-FeCN combined matrix we observed traces of RuO_4^- at a binding energy of 283 eV by XPS).[6a] This may be one of the reasons for missing information of the high-valent species in the earlier study.[11h] Apart from that, Ti-based supporting electrodes were not amenable for optical characterizations. On the other hand, in this work, direct UV−vis and IR measurements as well as electrochemical analyses revealed the presence of RuO_4^- in the ITO/Ru(VII)-RuO_x-CME film. Distinguishable optical characteristics with tunable redox properties are some interesting and new behaviors of the CME.

Sequential Step Preparation of RuO-FeCN. Typical CV responses of GCE/Ru(VII)-RuO_x-CME under two different conditional windows in pH 2 solution are given in Figure S2. Procedure for the sequential step RuO-FeCN-CME formation was as follows: (Step 1) Preparation of the Ru(VII)-RuO_x-CME under the optimal condition; (Step 2) the CME was washed with water and pH 2 solutions; (Step-3) Ru(VII)-RuO_x-CME was subjected to five repetitive CVs with 2 mM of $Fe(CN)_6^{3-}$ at a scan rate of v = 50 mV/s under condition I or II; (Step-4) the above CME was washed with water and pH 2; and (Step-5) CV was performed in blank pH 2 buffer solution. In order to get information about the nature of the ruthenium oxide redox species interaction with the $[Fe(CN)_6]^{3-}$, the Step 3 experiment is carried out discretely for two different conditional windows (conditions I and II) as shown in Figures S2(A)a and S2(B)a. Under condition II (≤1 V vs Ag/AgCl), the GCE/Ru(VII)-RuO_x-CME shows stable and well-defined peak response for the $Fe(CN)_6^{3-/4-}$ redox couple with equilibrium peak potential ($E_{1/2}$) and peak-to-peak separation (ΔEp) values of 290 mV and 69 mV, respectively (Step 3). Controlled experiments with GCE under an identical working condition yielded the value of ∼290 mV (observed 287 mV) and 72 mV, respectively, with lower peak current response (dotted line in Figure S2(A)). This observation indicates electronic and conducting behavior of the CME in the window [−0.1 to 1 V vs Ag/AgCl]. While the $E_{1/2}$ values of the $[Fe(CN)_6]^{3-/4-}$ redox couples at the CME and GCE surfaces are similar, an enhanced peak current response with the CME over the GCE is reminiscent of the participation of surface area effect rather than redox mediation with the CME system. The electrode was further transferred to blank solutions (Step 4), and then CV was measured (Step 5, Figure S2(A)b). Interestingly, there was no obvious alteration in the background response of the CME before and after $[Fe(CN)_6]^{3-}$ study, as witnessed by the stability of the electrode without any surface and redox site RuO_2 and RuO_3 interactions with the $[Fe(CN)_6]^{3-}$.[16] On the other hand, experiments under condition I (>1 V vs Ag/AgCl) with $[Fe(CN)_6]^{3-}$ resulted in a rapid decrease in the i_{pa}[3] response at 1.1 V vs Ag/AgCl, while the $[Fe(CN)_6]^{3-}$ response decrease slightly (Step 3, Figure S2(B)a). Extended experiment in Step 5 result in entirely different CV patterns as new three-redox peaks centered at 0 ($E^{o1'}$), 0.85 ($E^{o2'}$), and 1.05 ($E^{o3'}$) V vs Ag/AgCl corresponding to a RuO-FeCN-CME's characteristic response (Figure S2(B)b). The CV patterns closely matches with the RuO-FeCN film formed

by a mixture containing Ru^{3+} and $[Fe(CN)_6]^{3-}$ by a conventional E-cycle approach (Figure S3(A)).[5,6b] In other words, the high-valent redox species, RuO_4^- or RuO_4 with the CME under condition I selectively interacted with $Fe(CN)_6^{3-}$ for the new RuO-FeCN-CME formation. In order to further confirm the high-valent species participation within the RuO-FeCN, glucose oxidation catalysis was investigated as in Figure S2(B)c. As expected, it shows a defined electrocatalytic response at 1.1 V vs Ag/AgCl (1.44 V vs RHE) due to the high-valent RuO_4^- species. Finally, we also repeated the sequential RuO-MCN-CME formation with $[Ru(CN)_6]^{4-}$. The sequential procedure was successful in forming the corresponding RuO-RuCN-CME, similar to the classical preparation method, and also shows the glucose oxidation (Figure S2(C)). Control sequential formation experiments with other ruthenium oxide electrodes, such as E-cycle-prepared Ru(VII)-RuO_x-CME and RuO_x systems failed to show any such surface derivatizations. Possibly, the existence of very low concentration or the absence of the RuO_4^- species in the above systems was not able to produce any further surface derivatization. It should be noted that classical RuO_2 samples were often tested with $[Fe(CN)_6]^{3-}$, but never encountered any such surface derivation as mentioned above.[16] Hence, the tunable redox property of the Ru(VII)-RuO_x-CME along with optical and surface derivatization abilities are interesting and new features in this work.

Conclusions

Electrochemical oxidation of $RuCl_3$ at an applied potential of 1 V vs Ag/AgCl in pH 2 KCl-HCl buffer solution resulted in selective deposition of RuO_4^- along with protonated and hydrous nano forms of RuO_2 and RuO_3 (Ru(VII)-RuO_x-CME) on the underlying electrodes. The approach can be allowed for the formation of Ru(VII)-RuO_x-CME on non-Ti electrodes, such as GCE and ITO. The solid-state UV−vis pattern of ITO/Ru(VII)-RuO_x-CME matches very well with chemically generated RuO_4^- in alkaline conditions due to unusual formation and stabilization of the high-valent, RuO_4^- within the Ru(VII)-RuO_x-CME matrix. The Ru(VII)-RuO_x-CME selectively interacts with $[Fe(CN)_6]^{3-}$ or $[Ru(CN)_6]^{3-}$ at >1 V of working potential window (where the key species, RuO_4^-, gets activated), leading to the formation of respective polynuclear ruthenium oxide-hexacycnometallate films (RuO-MCN-CMEs). On the basis of this concept, a sequential based surface derivatization approach was successfully demonstrated for the RuO-MCN-CMEs formations. Ruthenium oxide electrodes with low concentration or absence of RuO_4^- were unsuccessful for the surface derivatization. Since the Ru(VII)-RuO_x-CME has interesting redox features along with optical property, the systems can be highly implicative for further synthetic inorganic methodologies and non-Ti-based RuO_2 electrode preparations and applications (electrochemical conductor and capacitor, etc.).

Acknowledgment. This work is partially supported by a Grant-in-Aid for Scientific Research from the Ministry of Education, Culture, Sports, Science, and Technology, Japan. A.S.K. gratefully acknowledges the Japan Society for the Promotion of Science (JSPS) for the postdoctoral fellowship and research grant. We also thank Dr. Jen-Lin Chang for the AFM analysis.

Supporting Information Available: Summary of the UV−vis data for various ruthenium oxide species and CMEs (Table S1), repetitive CV responses of the GCE/Ru(VII)-RuO_x-CMEs at different potential windows (Figure S1), detailed sequential formation of GCE/RuO-MCN-CME (M = Fe or Ru) from the GCE/Ru(VII)-RuO_x-CMEs by CV (Figure S2), and comparative CV responses of different type prepared GCE/RuO-FeCN-CMEs (Figure S3). This material is available free of charge via the Internet at http://pubs.acs.org.